READILY MADE COMPARISON AMONG THE THREE NEAR-FIELD MEASUREMENT GEOMETRIES USING A COMPOSITE NEAR-FIELD RANGE

Doren W. Hess
MI Technologies
4500 River Green Parkway
Duluth, Georgia 30096 U.S.A.
dhess@mi-technologies.com

ABSTRACT

In this paper I demonstrate how our current technology now very readily permits a standard of accuracy and utility to be realized, that was formerly available only in research laboratories. This is accomplished with standardly available positioning equipment and standardly available software. Accurate alignment of the range is enabled by a tracking laser interferometer. This composite near-field scanning antenna range has afforded us the opportunity to compare readily, far-field results from the classic planar, cylindrical and spherical coodinate systems. Comparison data are presented.

Keywords: Antenna Metrology , Near-Field Antenna Measurements, Planar Near-Field Scanning, Cylindrical Near-Field Scanning, Spherical Near-Field Scanning

1.0 Introduction

Over the past year we at MI Technologies have carried out a measurement study which culminated in a comparison of far-field pattern results among the three most common geometries. The results reveal excellent agreement among the three methods. In this paper I demonstrate how our current technology now very readily permits a measurement capability to be realized, formerly available only in research laboratories. Unlike the systems built for experimental purposes and systems built under special engineering projects, this system was assembled from positioners that are catalog products. The corresponding planar, cylindrical and spherical near-field to far-field (NFFF) transform software modules that were used in this work are also catalog items.

2.0 The Composite Near-Field Scanning System

This composite near-field scanning system is composed of two major positioning subsystems: an X-Y- planar scanner and a Roll-over-Azimuth spherical positioner. When integrated together, it forms a near-field scanning system capable of three types of near-field measurement techniques – planar, cylindrical and spherical -- near-field scanning.

The X-Y- scanner includes provision for rotating the probe in polarization about its z-axis. This system has a total of five active axes that it controls. At any one time it controls the two step-scan motions of the probe over the measurement surface, augmented by its control of probe polarization. This entails control over three axes. The other two axes are set and can be held to defined fixed positions while the scanning motion is executed. Similar systems have been built that have probe z-translation and auxiliary AUT z-translation as well.

The order of alignment is as follows:

a) Internal Alignment of X-Y- Scanner for Straightness and Orthogonality and for Orthogonality of the Probe Polarization axis to the scan plane
b) Internal Alignment of the Roll/Azimuth Scanner for Intersection Distance and Orthogonality
c) Relative Alignment of the Roll/Azimuth Scanner and the X-Y- Scanner to set the vertical Y-axis of the X-Y- scanner and the vertical Azimuth axis of the Roll/Azimuth positioner parallel in each of two vertical planes. See Figure 3 for an illustration.
d) Alignment of the probe horn's cylinder axis to the X-Y- scan plane and its polarization positioner
e) Alignment of the antenna-under-test to the roll axis of the spherical scanner

The composite system was aligned mechanically using a tracking laser interferometer system. A key aspect of the success of the results reported here is the care devoted to this alignment before any data were acquired. The computerized tracking laser makes short work of the alignment steps that used to require much more tedious optical methods.

The same open ended rectangular waveguide probe was used for each of the three measurements. It's pattern was estimated by use of the Yaghjian model. Probe pattern correction was employed in each of the three measurements although no calibration measurements per se of probe patterns were needed.

3. The Planar Near-Field Subsystem

A schematic of planar near-field scanning and a photograph of the X-Y- scanner used in these measurements are shown in Figures 1 and 2 below.

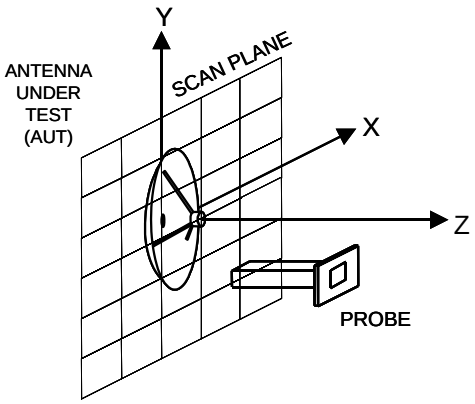

Figure 1. Schematic of Planar Near-Field Scanning

Figure 2. Photograph of Planar Near-Field Scanner

The scanner has a 36 inch square scan area and a Z-positional accuracy of approximately +/- 0.0015 inches, worst case. It is entirely covered with absorber when in use. It is outfitted with a probe polarization and probe Z-axis.

4. The Spherical Near-Field Subsystem

A schematic of spherical near-field scanning and a photograph of the Roll/Azimuth scanner used in these measurements are shown in Figures 3 and 4 below.

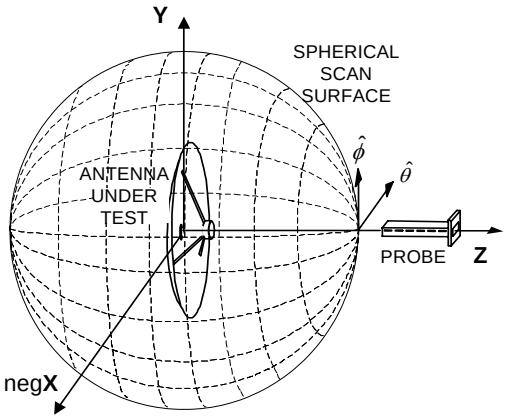

Figure 3. Schematic of Spherical Near-Field Scanning

Figure 4. Photograph of a Roll-over-Azimuth Spherical Near-Field Positioning Subsystem Without Absorber

The Roll axis is located 42 inches above the floor. The antenna used in this work is depicted here, along with the utility alignment hardware The throat of the offset arm can accommodate up to a 36 inch diameter dish. The intersection distance is less than 0.005 inches.

5. The Cylindrical Near-Field Subsystem

Schematics of cylindrical near-field scanning and a schematic of the cylindrical near-field positioning subsystem used in these measurements are shown in Figures 5 and 6 below.

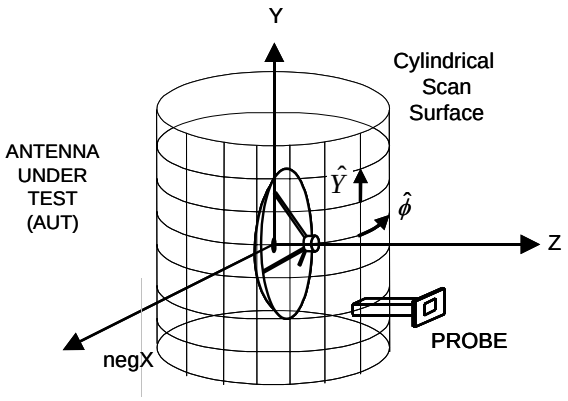

Figure 5. Schematic of Cylindrical Near-Field Subsystem

Cylindrical scanning makes use of the Azimuth of the spherical scanner and the vertical Y- axis of the X-Y-scanner. Achieving parallelism between these two axes in each of two vertical planes is critical for good alignment of the cylindrical range.

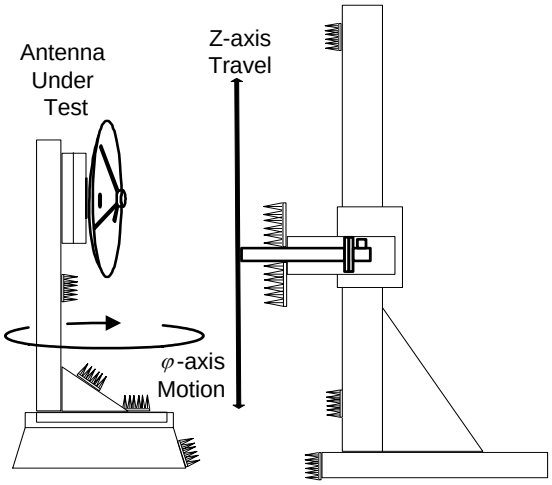

Figure 6. Schematic of Cylindrical Near-Field Positioning Subsystem as Assembled from Planar and Spherical Near-Field Scanners

The distance between the aperture of the probe antenna and the azimuth axis was 38.5 inches, which then determined the radius of the measurement cylinder and the radius of the measurement sphere.

6. Layout and Setup of the Range

The range was located in an area 20 ft in length and 12 ft in width; it occupied a corner of a larger 20 ft square room. The ceiling height of the facility is 96 inches above the floor. The height of the range axis – the Roll axis and the center of the scan plane - was 42 inches above the floor. Eight-inch pyramidal absorber was used in specular regions on the floor, the corner walls and the ceiling. Absorber was also placed over the exposed metal surfaces of the positioning equipment. The range was aligned by first installing the planar scanner in the corner area and then installing the Roll/Azimuth spherical scanner so that the Azimuth and Y- axes were nominally vertical but accurately parallel. The Azimuth axis was shimmed and bolted to the concrete floor. The X-Y-scanner was assumed to be sufficiently stable that no anchoring was needed.

In the measurements reported here no realignments of the axes between measurements in the three scanning coordinate systems were made. The test antenna was aligned only once -- to the roll axis of the SNF scanner by use of a mirror on the back of the antenna; the antenna's alignment mirror had been set so that its normal lay in the same direction as the axis of its main beam. As a result of this antenna alignment and the range alignment, the main beam peak was measured to lie at range boresight in each of the three coordinate systems.

The antenna used for this demonstration was the original pattern standard antenna from MI's earlier Scientific-Atlanta era of the 1980's. It is a ruggedized reflector antenna that has been specially designed and preserved as a reference for such comparison measurements. The diameter of the dish is 67.3 cm (26.5 inches). It is fed by simple rectangular pyramidal horn that is linearly polarized. The operating frequency of this antenna is 13.00 GHz.

For the cases of planar and cylindrical scanning, the amounts of near-field pattern coverage available on this system was rather limited when compared to the usual research laboratory environment. The PNF scanner had a maximum travel of 36 inches in X and Y and consequently the CNF scanner had a maximum vertical axis travel of 36 inches. This then limited the far-field pattern coverage one could expect according to the truncation rules for planar and cylindrical scanning. At the separation distance of 38.5 inches where the scanners were set up for these measurements, the corresponding far-field coverage was just less than ±10 degrees: i.e. from the truncation rule

$$\pm \theta_C = \pm \tan^{-1}[(L-D)/2d] = \pm \tan^{-1}[(36''-24'')/(2 \times 38.5'')]$$

$$\pm\theta_C = \pm 9 \text{degrees}$$

where L is the length of the scan, D is the diameter of the test antenna and d is the distance from the probe to the azimuth axis.

7. Comparison of Results

The comparison exhibited here then is limited to that far-field region only. Please refer to Figures 8, 9 and 10. Each of the three contours is derived from a different form of near-field antenna measurement -- planar, cylindrical, spherical – made on the same antenna in the demonstration room at the MI technologies River Green facility. The 4 dB contours span a dynamic range of 60 dB and a coverage area of ± 10 degrees about the main beam .

The overall resemblance among the patterns is evident to the viewer and there is no doubt that the three patterns are nearly the same. The reader may notice some discrepancies among the three contours. This is not unexpected. Such discrepancies arise because of stray reflection signals, approximations in modeling the probe and positioner alignment uncertainties. These types of error contributions are present in any antenna measurement. Controlling them is critical to successful near-field measurements. The facility where the data was taken was partially treated with absorber to handle the main beam region of the test antenna. The stray signals were controlled in this environment only down to approximately a –35 dB reflectivity level.

8. Discussion

The pattern agreement tends to validate the measurement system and each of its components as qualified for near-field applications. Quantifying this however requires an analysis of the discrepancies. An overlay of three pattern cuts from Figures 8, 9 & 10, through the main beam peak, is shown in Figure 7. Here, the amount of disagreement can be discerned for use in analyzing the level of discrepancies. See the illustration below to understand the phasor relationship between the true sidelobe level $\mathbf{E_O}$ and the perturbed sidelobe level $\mathbf{E_O+E_S}$ that has been affected by the stray signal $\mathbf{E_S}$. For example 1 dB of

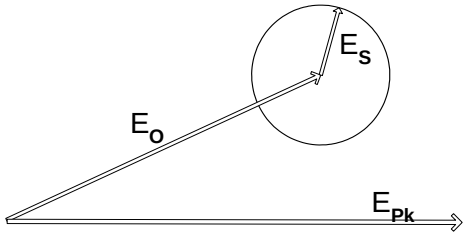

pattern

discrepancy at a level of –25 dB corresponds to an equivalent stray signal of –50 dB. In Figure 7 at a pattern angle of –4.5 degrees one can identify a peak-peak pattern discrepancy of 2 dB, at a level on the stronger pattern of –23.5 dB.
The equation below

$$20\log\frac{E_S}{E_{Pk}} = 20\log\frac{E_2}{E_{Pk}} + 20\log\left[\frac{1-10^{-\Delta/20}}{2}\right]$$

then yields an equivalent stray signal level of –23.5 –19.8 = -43.3 dB, where Δ is the peak-to-peak discrepancy (E_2-E_1 **)** of 2 dB and E_2 is the stronger of the two sidelobe levels E_1 the weaker.

The gain of the reflector antenna was measured in each of the three coordinate systems by the range insertion loss technique. No account of impedance mismatch error has been made. The pad attenuator used had an attenuation value of 20.01 dB as measured with a network analyzer. The additional cable loss was approximately 1.2 dB, which needs to be included in the attenuation value. The measured gain for the reflector antenna in each case is tabulated below:

Measured Gain Values –Reflector Antenna	
Planar Near-Field	33.2 dB
Cylindrical Near-Field	33.5 dB
Spherical Near-Field	34.0 dB
Estimated Accuracy	±1.0 dB

This antenna has been measured earlier in the 1982-3 timeframe using spherical near-field and compact range techniques. The results were reported at AMTA 1983. The value of gain reported then was 33.8 dB ± 0.6 dB. The measurements reported here are consistent with those earlier measured values of gain.

The lack of excellent and precise repeatability of the gain measurements was due to the modest level of care and expense we elected to take in making the range insertion loss and probe pattern measurements. Better and more accurate gain measurements can be made if required.

9. Summary

In summary, we have demonstrated the ease with which near-field comparison measurements can be made by exhibiting planar, cylindrical and spherical near-field pattern and gain results made on a system composed of an X-Y- scanner and a Roll/Azimuth positioner.

10. ACKNOWLEDGMENTS

Many others before me – too many to reference easily -- have built antenna ranges capable of more than one form of near-field scanning. The author greatly appreciates the support he received from the MI Technologies staff –the clever system engineering advice from Mr. Donald Weiss and encouragement from Mr. Jeff Fordham.

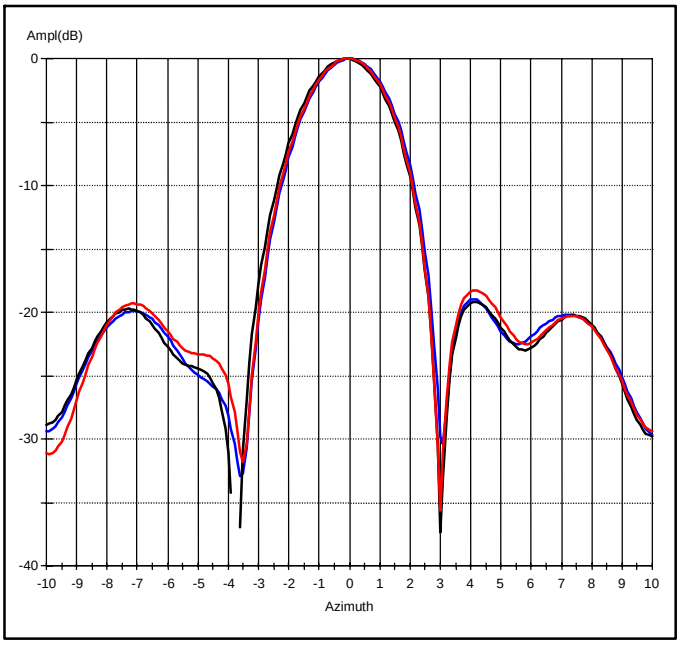

Figure 7. Overlay of Azimuth Cut For Planar, Cylindrical, and Spherical Results.

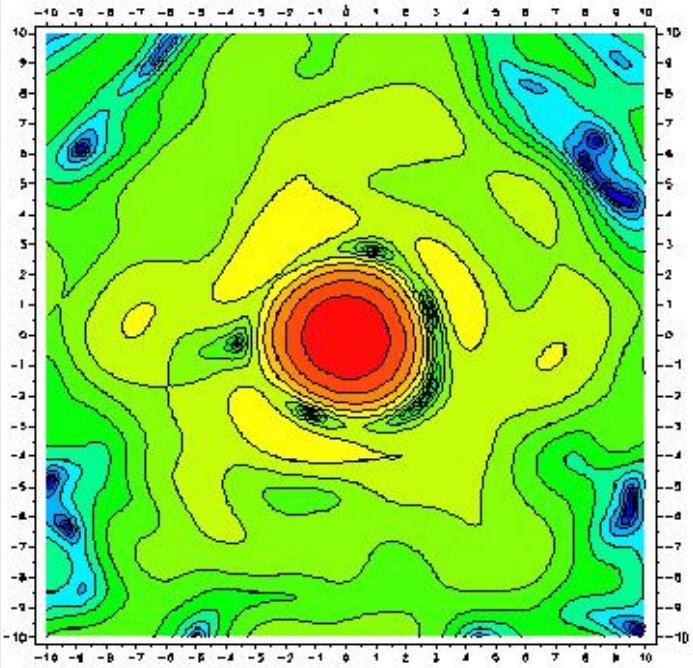

Figure 8.

Planar Near-Field Result

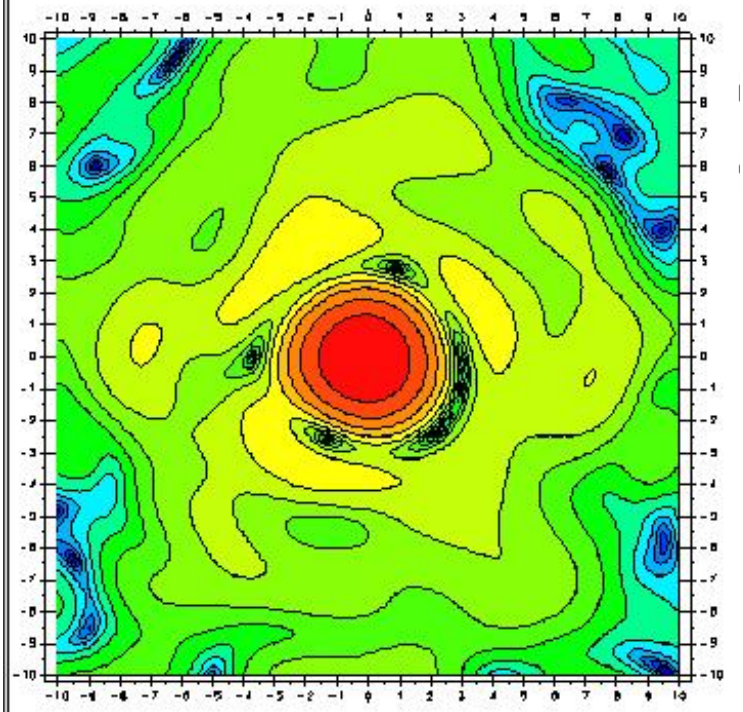

Figure 9

Cylindrical Near-Field Result

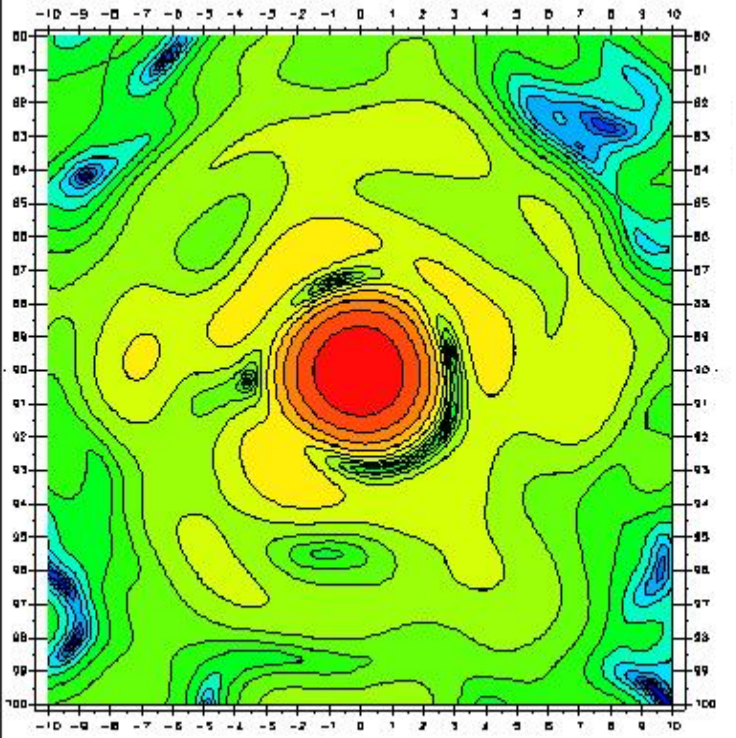

Figure 10

Spherical Near-Field Result